Laser acceleration of electrons in vacuum

Eric Esarey, Phillip Sprangle, and Jonathan Krall
Beam Physics Branch, Plasma Physics Division, Naval Research Laboratory, Washington, D.C. 20375-5346
(Received 9 May 1995)

Several features of vacuum laser acceleration are reviewed, analyzed, and discussed, including electron acceleration by two crossed laser beams and acceleration by a higher-order Gaussian beam. In addition, the vacuum beat wave accelerator (VBWA) concept is proposed and analyzed. It is shown that acceleration by two crossed beams is correctly described by the Lawson-Woodward (LW) theorem, i.e., no net energy gain results for a relativistic electron interacting with the laser fields over an infinite interaction distance. Finite net energy gains can be obtained by placing optical components near the laser focus to limit the interaction region. The specific case of a higher-order Gaussian beam reflected by a mirror placed near focus is analyzed in detail. It is shown that the damage threshold of the mirror is severely limiting, i.e., substantial energy gains require very high electron injection energies. The VBWA, which uses two copropagating laser beams of different frequencies, relies on nonlinear ponderomotive forces, thus violating the assumptions of the LW theorem. Single-particle simulations confirm that substantial energy gains are possible and that optical components are not needed near the focal region.

PACS number(s): 41.75.Lx, 41.75.Ht, 42.62.Hk, 52.40.Nk

I. INTRODUCTION

In recent years there has been a renewed interest in the possibility of accelerating electrons by laser fields in vacuum [1–6]. This is partly due to the development of ultrahigh power ($\geq$ 10 TW), short pulse ($\leq$ 1 ps), tabletop lasers based on chirped-pulse amplification [7,8]. A large portion of laser-driven electron acceleration research has focused on plasma-based schemes such as the plasma beat wave accelerator [9,10] and the laser wake field accelerator [10–12]. Although plasma-based schemes can achieve ultrahigh acceleration ($\geq$ 10 GV/m) and offer the possibility of guiding the laser pulse (preventing pulse diffraction), they suffer from several difficulties including laser-plasma instabilities, plasma uniformity requirements, and electron beam-plasma collisions. Laser acceleration in vacuum can eliminate the difficulties associated with the plasma. In this article we will (i) discuss some general features and characteristics of laser acceleration in vacuum, including what has become known as the Lawson-Woodward (LW) theorem [13–15]; (ii) analyze electron acceleration using two crossed laser beams in vacuum, which was the subject of recent papers [4,5]; (iii) discuss and analyze electron acceleration by a higher-order Gaussian mode in vacuum; (iv) quantify certain limitations on acceleration imposed by the damage threshold of optical components; and (v) propose and analyze a vacuum laser acceleration concept called the vacuum beat wave accelerator.

A major difficulty in using laser fields in vacuum to accelerate electrons is that the phase velocity of the electric field in the direction of the accelerated electrons is greater than c for a focused laser beam. For example, consider a transversely polarized laser field propagating in the z direction with a Gaussian radial profile. Since the electric field $\mathbf{E}$ is radially bounded, $\nabla\cdot\mathbf{E}=0$ implies a finite E_z component that can accelerate electrons traveling in the z direction. The phase velocity v_p of the E_z field is given approximately by $v_p/c\simeq 1+1/(kZ_R)$, where $\omega=ck$ is the laser frequency, $Z_R=kw_0^2/2$ is the Rayleigh length, which is the characteristic distance over which the laser spot size $w(z)$ expands, $w=w_0(1+z^2/Z_R^2)^{1/2}$, and w_0 is the minimum spot size of the laser beam at focus. In effect, the vacuum dispersion relation is given by $\omega^2/c^2=k_z^2+4/w_0^2$, where k_z is the axial wave number and $v_{\rm ph}\simeq\omega/k_z$. Since $v_p>c$, relativistic electrons with $v_z\simeq c$ will phase slip with respect to E_z and will eventually decelerate. This will occur over a slippage distance z_s, defined to be the distance over which a relativistic electron phase slips by π, $kz_s|v_z/c-v_{\rm ph}/c|\simeq\pi$, which gives $z_s\simeq\pi Z_R$. If the electron interacts over a distance large compared to the slippage distance $z\gg z_s$, the accelerating and decelerating regions tend to cancel, resulting in a very little net energy gain. In fact, one can show that if an electron with $v\simeq c$ interacts with a laser field in vacuum over an infinite region ($z=-\infty$ to ∞), the net energy gain is zero. This is the main point of the so-called LW theorem [13–15].

Recently, a vacuum laser acceleration configuration that uses two crossed laser beams was discussed and analyzed [4,5]. Here the first and second beams propagate at angles of θ and $-\theta$ with respect to the z axis such that their focal points intersect at the origin ($z=0$) as shown in Fig. 1. The two lasers have the same frequency and are phased such that the transverse electric fields cancel on axis while the axial fields add. Properly phased electrons injected along the z axis can be accelerated by the net axial component of the laser field. However, a highly relativistic electron traveling along the z axis from $-\infty$ to $+\infty$ will experience both accelerating and decelerating phase regions of the laser field. In fact, analysis indicates that the net energy gain vanishes over an infinite interaction region [5], which is in agreement with the LW theorem, contrary to the claims of Ref. [4].

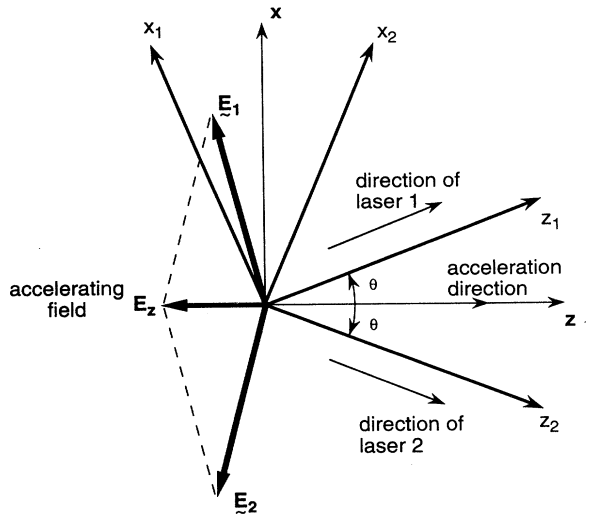

FIG. 1. Coordinate system and electric fields for two crossed laser beams.

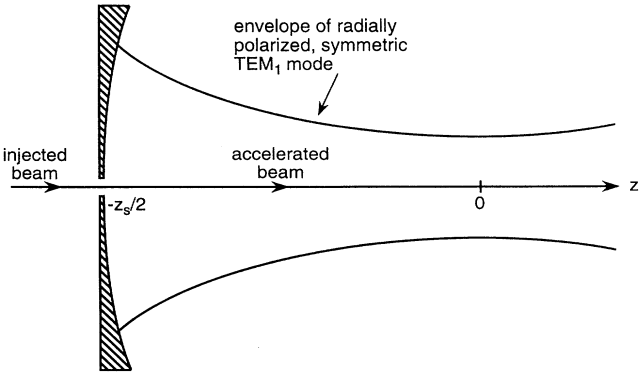

FIG. 2. Schematic of electron acceleration by reflecting a higher-order Gaussian beam from a mirror placed near focus.

One or more of the assumptions of LW theorem [13–15] must be violated in order to achieve a nonzero net energy gain by using laser fields in vacuum. The LW theorem assumes that (i) the laser fields are in vacuum with no walls or boundaries present, (ii) the electron is highly relativistic ($v \simeq c$) along the acceleration path, (iii) no static electric or magnetic fields are present, (iv) the region of interaction is infinite, and (v) ponderomotive effects (nonlinear forces, e.g., the $\mathbf{v}\times\mathbf{B}$ force) are neglected. For example, finite energy gains can be achieved by introducing a background of gas into the interaction region, as in the inverse Cherenkov accelerator [16,17]. Physically, the gas reduces the phase velocity of the laser such that $v_p \leq c$, reducing the slippage. Alternatively, acceleration can result from the introduction of a periodic magnetic wiggler field, as in the inverse free electron laser [18–24]. In vacuum, a nonzero energy gain can be achieved by the introduction of optical components that limit the interaction distance to a finite region about the laser focus. Typically, the optimal length of this region is the slippage distance z_s. An example of such a configuration is shown in Fig. 2, in which a mirror placed near the focal point reflects a higher-order Gaussian mode.

Although finite energy gains can be achieved in principle by limiting the interaction distance to a slippage distance, this may be difficult to realize in practice due to limitations imposed by the damage threshold of the optical components. If the laser-electron interaction distance is limited to approximately z_s, it is possible to show that the maximum energy gain $\Delta W_{\max}$ of the electron is $\Delta W_{\max}(\mathrm{MeV}) \simeq C_0[P(\mathrm{TW})]^{1/2}$, where P is the laser power in TW and C_0 is a constant. Typically, C_0 is in the range 20–30, depending on the specific laser geometry. The damage threshold of the optical components used to limit the interaction distance is characterized by a critical intensity I_d. Typically, for a 1-ps laser pulse, $I_d \leq 5$ TW/cm^2 [25]. Since the slippage distance is typically on the order of a Rayleigh length $z_s \simeq \pi Z_R$, the optical components must be placed relatively close to the focal point. This implies that the intensity at the surface of the optics is given by $I_s \simeq P/(\pi w_0^2)$. Hence, for a fixed laser power P, the surface intensity can be reduced such that $I_s < I_d$ simply by increasing the focal spot size w_0. Naively, one might assume that this would not affect the total energy gain of the electron, since $\Delta W_{\max}$ depends only on the laser power P. This, however, is not the case. As the spot size increases, the phase velocity of the accelerating field decreases such that $v_{\mathrm{ph}} \to c$. Phase slippage, which limits the acceleration distance, is then dominated by the initial electron injection energy and not by diffraction, as previously assumed. The result $\Delta W_{\max}(\mathrm{MeV}) \simeq C_0[P(\mathrm{TW})]^{1/2}$ only applies if the initial electron injection energy W_I is above a critical value W_c. Typically, $W_c(\mathrm{MeV}) \simeq w_0/\lambda$, where λ is the laser wavelength. Hence, increasing w_0 increases W_c. For example, $\lambda = 1$ μm, $P = 10$ TW, and $I_d = 5$ TW/cm^2 imply $w_0 > 0.8$ cm and $W_c > 9$ GeV. For $W_I \ll W_c$, both the slippage distance and the maximum energy gain are greatly reduced, i.e., $z_s \ll Z_R$ and $\Delta W_{\max} \simeq C_0 P^{1/2}(W_I/W_c)^2$. For $\lambda = 1$ μm, $P = 10$ TW, $I_d = 5$ TW/cm^2, and $W_I = 1$ GeV, the maximum energy gain is $\Delta W_{\max} \sim 1$ MeV.

Laser acceleration of electrons in vacuum can be realized using the nonlinear or ponderomotive forces associated with the laser-electron interaction. The LW theorem assumes that the electron is traveling with $v = c$ and that the velocity is unaffected by the laser fields. Ponderomotive forces arise by considering the effect the laser field has on the electron trajectory. Consider one or more laser beams propagating in along the z axis, which interact with a relativistic electron traveling along the z axis. The rate of change of the electron energy gain is determined by the term $\mathbf{v}\cdot\mathbf{E}$, where $\mathbf{v}$ is the electron velocity. Typically, vacuum acceleration schemes are concerned with the term $v_z E_z$, where $v_z \simeq c$, such that the energy gain is determined by the integral $\int dz\, E_z$. The LW theorem, as discussed in Sec. II, specifically addresses this case. If the transverse electric field $E_\perp$ of the laser is finite along the z-axis, a transverse velocity $v_\perp$ will be in-

troduced. In the one-dimensional limit ($w_0 \gg \lambda$), conservation of canonical momentum implies $v_\perp \simeq eA_\perp/(\gamma mc^2)$, where $A_\perp$ is the vector potential, $E_\perp = -(1/c)\partial A_\perp/\partial t$, and $\gamma = (1-v^2/c^2)^{-1/2}$ is the relativistic factor of the electron. Hence $\mathbf{v}_\perp \cdot \mathbf{E}_\perp \sim (1/\gamma)\partial A_\perp^2/\partial t$. This term, which is unaccounted for in the LW theorem, is responsible for changes in the electron energy due to nonlinear, "ponderomotive" effects. The use of ponderomotive forces can result in substantial energy gains even in the limit of an infinite interaction region. Hence optical components are not required near (within a few Z_R) the laser focus.

In Sec. V we propose and analyze a vacuum beat wave accelerator (VBWA), which relies on the ponderomotive acceleration resulting from the beat wave produced by the interaction of two laser beams. In the VBWA, two laser beams of different frequencies are copropagated in the presence of an injected electron beam, as shown in Fig. 3. Properly phased electrons, traveling essentially along the same axis as the two laser beams, experience an axial acceleration from the beat term in the $\mathbf{v}\times\mathbf{B}$ force. By properly choosing the frequencies, focal spot sizes and/or the focal points of the two beams, the phase velocity of the beat wave can be adjusted such that $v_{\rm ph} \leq c$. Hence the phase velocity can be tuned to the electron velocity and the problem of phase slippage can be reduced. The acceleration mechanism in the VBWA is similar to that of the inverse free-electron laser (IFEL) [18–24]. In effect, the wiggler field in the IFEL is replaced by one of the lasers in the VBWA.

The remainder of this paper is organized as follows. Section II presents a discussion of LW theorem. Electron acceleration in vacuum by using two intersecting laser beams is analyzed in Sec. III. Specifically, it is shown that the results of the LW theorem apply to this configuration. Vacuum acceleration by a higher-order Gaussian mode is discussed and analyzed in Sec. IV. The importance of the injection energy W_I being greater than the critical energy W_c is emphasized. Limitations due to the damage threshold of optical components are discussed in Sec. V. It is shown that if optical components are required within a Rayleigh length Z_R of focus, then increasing the focal spot size to avoid damage implies a large value for the critical energy W_c. If $W_I \ll W_c$, the energy gain will be reduced by the factor $W_I^2/W_c^2 \ll 1$. In Sec. VI the VBWA is proposed and analyzed. This includes single-particle simulations based on model equations that describe the electron motion. The paper concludes with a discussion in Sec. VII.

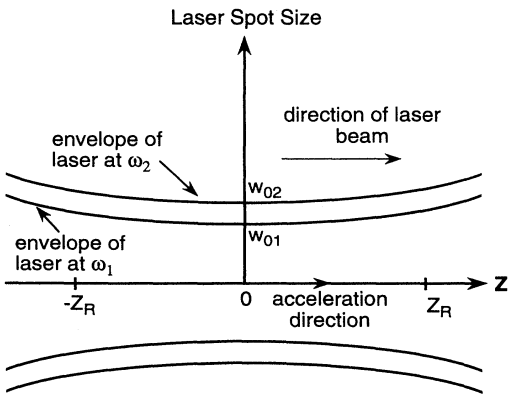

FIG. 3. Schematic of the vacuum beat wave accelerator configuration.

II. LAWSON-WOODWARD THEOREM

The LW theorem states that, under certain conditions, the net energy gain of a relativistic electron interacting with an electromagnetic field in vacuum is zero [13–15]. The theorem assumes that (i) the laser field is in vacuum with no walls or boundaries present, (ii) the electron is highly relativistic ($v \simeq c$) along the acceleration path, (iii) no static electric or magnetic fields are present, (iv) the region of interaction is infinite, and (v) ponderomotive effects (nonlinear forces, e.g., the $\mathbf{v}\times\mathbf{B}$ force) are neglected. Given the above assumptions, the lack of an energy gain can be shown [1] by considering the vacuum wave equation $\nabla^2\mathbf{E} = -(\omega/c)^2\mathbf{E}$, where ω is the frequency. For a relativistic electron moving in the z direction $v_z \simeq c$, the acceleration is due to the E_z component, which is given by

$$E_z = (2\pi)^{-1}\int dk_x \int dk_y \hat{E}_z(k_x,k_y) \times \exp[i(k_x x + k_y y + k_z z - \omega t)] , \tag{1}$$

where $\hat{E}_z(k_x,k_y)$ is the Fourier amplitude and $k_z = (\omega^2/c^2 - k_x^2 - k_y^2)^{1/2}$ is the vacuum dispersion relation. Electromagnetic fields in vacuum satisfy $\nabla\cdot\mathbf{E}=0$, which implies $\hat{E}_z = -(k_x\hat{E}_x + k_y\hat{E}_y)/k_z$. Without loss of generality, $\hat{E}_y = 0$ is assumed. For a highly relativistic electron moving along the z axis, i.e., $x = y = 0$ and $t = z/c$, the total energy gain is proportional to

$$\int_{-\infty}^{\infty} dz\, E_z = -\int dk_x \int dk_y (k_x/k_z)\hat{E}_x(k_x,k_y) \times \delta(k_z - \omega/c) . \tag{2}$$

By introducing a change of variables $k_x = k_\perp\cos\phi$ and $k_y = k_\perp\sin\phi$, where $\int dk_x \int dk_y = \int d\phi \int dk_\perp k_\perp$ and $\delta(k_z - \omega/c) = (k_z/k_\perp)\delta(k_\perp)$, it is clear that

$$\int_{-\infty}^{\infty} dz\, E_z = -\int d\phi \int dk_\perp (k_\perp\cos\phi) \times \hat{E}_x(k_\perp\cos\phi, k_\perp\sin\phi)\delta(k_\perp) = 0 , \tag{3}$$

assuming $k_\perp\hat{E}_x \to 0$ as $k_\perp \to 0$. Hence there is no net energy gain.

In order to achieve a nonzero energy gain by using laser fields in vacuum, one or more of the assumptions in the LW theorem must be violated. For example, a finite interaction region (on the order of a few Z_R) can be considered. However, this may be difficult to achieve in practice due to the high-intensity requirement on the laser field and the damage threshold limitations of optical components, as discussed in Sec. V. Alternatively, one

can rely on nonlinear forces to produce the desired acceleration, such as the ponderomotive force associated with the $\mathbf{v}\times\mathbf{B}$ term. This can lead to substantial energy gains even in the limit of an infinite interaction region. An example of an accelerator based on the nonlinear ponderomotive force is the vacuum beat wave accelerator, which is discussed Sec. VI.

III. TWO CROSSED LASER BEAMS

Recently, a vacuum laser acceleration configuration was discussed and analyzed [4,5]. In this scheme a pair of linearly polarized laser beams with Gaussian profiles, having the same frequency, are focused and intersected in vacuum, as shown in Fig. 1. Here the first laser propagates along the z_1 axis and the second laser propagates along the z_2 axis, where the z_1 axis and the z_2 axis are rotated by angles of θ and $-\theta$, respectively, with respect to the z axis. The phases of the lasers are such that the transverse electric fields cancel on axis while the axial fields add. Properly phased electrons injected along the z axis can be accelerated by the net axial component of the laser field. However, a highly relativistic electron traveling from $z=-\infty$ to ∞ will experience both accelerating and decelerating phase regions of the laser field. In fact, the net energy gain vanishes over an infinite interaction region [5], which is in agreement with the LW theorem, contrary to the claims of Ref. [4].

The axial electric field associated with the intersecting laser beams can be calculated by writing the laser fields in the (x,y,z) coordinate frame. In the (x_1,y_1,z_1) coordinate frame, where $x_1=x\cos\theta-z\sin\theta$, $y_1=y$, and $z_1=z\cos\theta+x\sin\theta$, the electric field of the first laser beam consists of a transverse and longitudinal component $\mathbf{E}_1=E_{x1}\mathbf{e}_{x1}+E_{z1}\mathbf{e}_{z1}$, where $\mathbf{e}_{x1}$ and $\mathbf{e}_{z1}$ are unit vectors. In the paraxial approximation ($\lambda\ll w_0$), the electric field components of a Gaussian laser beam are given by [26]

$$E_{x1}=\frac{E_{01}w_0}{w_1}\exp\left[-\frac{r_1^2}{w_1^2}\right]\cos\psi_1\ , \tag{4a}$$

$$E_{z1}=\frac{2E_{01}x_1}{kw_1^2}\exp\left[-\frac{r_1^2}{w_1^2}\right]\left[\sin\psi_1-\left[\frac{z_1}{Z_R}\right]\cos\psi_1\right]\ , \tag{4b}$$

where the phase of the transverse field E_{x1} is

$$\psi_1=kz_1-\omega t+z_1r_1^2/(Z_Rw_1^2)-\tan^{-1}(z_1/Z_R)+\phi_0\ , \tag{5}$$

E_{01} is the maximum field amplitude, $w_1=w_0(1+z_1^2/Z_R^2)^{1/2}$ is the laser spot size, w_0 is the minimum spot size (waist), $Z_R=\pi w_0^2/\lambda$ is the Rayleigh length, $\lambda=2\pi c/\omega$ is the wavelength, $\omega=ck$ is the frequency, k is the wave number, $r_1=(x_1^2+y_1^2)^{1/2}$, and ϕ_0 is a constant. The longitudinal field component in Eq. (4b) is necessary for the field to be divergence free, i.e., a physically realizable vacuum electromagnetic field. This important field component is not considered in Ref. [4]. In obtaining Eq. (4b) it was assumed that $w_0\gg\lambda$, which is consistent with the paraxial approximation. The field components for the second laser beam are given by Eqs. (4a) and (4b) with the subscript 1 replaced by 2.

The total transverse E_x and axial E_z components of the combined laser fields in the (x,y,z) coordinate frame are $E_x(x,y,z,t)=(E_{x1}+E_{x2})\cos\theta+(E_{z1}-E_{z2})\sin\theta$ and $E_z(x,y,z,t)=-(E_{x1}-E_{x2})\sin\theta+(E_{z1}+E_{z2})\cos\theta$. In order to have only an axial field component along the z axis ($x=y=0$), we set $E_{01}=-E_{02}=E_0$, such that $E_{x1}=-E_{x2}$ and $E_{z1}=E_{z2}$. This gives $E_x(0,0,z,t)=0$ and

$$\begin{aligned}E_z(0,0,z,t)&=-\frac{2E_0\sin\theta}{(1+\hat{z}^2\cos^2\theta)^{3/2}}\exp\left[-\frac{(\hat{z}/\theta_d)^2\sin^2\theta}{(1+\hat{z}^2\cos^2\theta)}\right](\cos\psi+\hat{z}\cos\theta\sin\psi)\\&=-\frac{2E_0\sin\theta}{(1+\hat{z}^2\cos^2\theta)}\exp\left[-\frac{(\hat{z}/\theta_d)^2\sin^2\theta}{(1+\hat{z}^2\cos^2\theta)}\right]\cos\psi_t\ ,\end{aligned} \tag{6}$$

where

$$\psi=kz\cos\theta-\omega t+\frac{\hat{z}^3\cos^3\theta\tan^2\theta}{\theta_d^2(1+\hat{z}^2\cos^2\theta)}-\tan^{-1}(\hat{z}\cos\theta)+\phi_0\ , \tag{7}$$

$\psi_t=\psi-\tan^{-1}(\hat{z}\cos\theta)$, $\hat{z}=z/Z_R$, and $\theta_d=w_0/Z_R$ is the diffraction angle. For small intersection angles $\theta\ll1$, the axial accelerating field in Eq. (6), acting upon an electron traveling with velocity $v_z\simeq c$, is

$$E_z=-\frac{2E_0\theta}{(1+\hat{z}^2)}\exp\left[-\frac{(\hat{z}\theta/\theta_d)^2}{(1+\hat{z}^2)}\right]\cos\psi_t\ , \tag{8}$$

where

$$\psi_t\simeq-\theta_d^{-2}\int d\hat{z}/\gamma_z^2-\hat{z}(\theta/\theta_d)^2/(1+\hat{z}^2)-2\tan^{-1}\hat{z}+\phi_0\ , \tag{9}$$

$t=\int dz/v_z$ has been assumed, $v_z/c\simeq1-1/2\gamma_z^2$, and $\gamma_z=(1-v_z^2/c^2)^{-1/2}$.

The phase velocity $v_{\rm ph}$ of the accelerating field in Eq. (8) is greater than c and therefore slips ahead of the electron. The expression for ψ_t in the limit $\theta^2\ll1$ implies

$$\frac{v_{\rm ph}}{c}=\left\{1-\left[\frac{(1-\hat{z}^2)\theta^2+2(1+\hat{z}^2)\theta_d^2}{2(1+\hat{z}^2)^2}\right]\right\}^{-1}\ . \tag{10}$$

Near the focal point $|z|\lesssim Z_R$,

$$v_{\rm ph}/c \simeq 1+(\theta^2+2\theta_d^2)/2=1+1/(2\gamma_c^2)\ , \tag{11}$$

where $\gamma_c=(\theta^2+2\theta_d^2)^{-1/2}$ defines a critical energy. The slippage distance z_s, defined as the distance required for the electron to phase slip by π, can be estimated by $\omega z_s|v_{\rm ph}^{-1}-v_z^{-1}|\simeq\pi$, i.e.,

$$z_s \simeq \gamma_c^2\lambda/(1+\gamma_c^2/\gamma_z^2)\ . \tag{12}$$

In the high-energy limit $\gamma_z \gg \gamma_c$, slippage is dominated by diffraction, i.e., the second and third terms in Eq. (9). In the low-energy limit $\gamma_z \ll \gamma_c$, slippage is dominated by the low velocity of the electron, i.e., the first term in Eq. (9). In the low-energy limit ($\gamma_z \ll \gamma_c$), the slippage distance $z_s \simeq \gamma_z^2\lambda \ll Z_R$ is much less than Rayleigh length, while in the high-energy limit ($\gamma_z \gg \gamma_c$), the slippage distance $z_s \simeq \lambda/(\theta^2+2\theta_d^2)$ can be comparable to a Rayleigh length. The critical energy $W_c=(\gamma_c-1)mc^2$ for the parameters in Ref. [4] is $W_c \simeq 4$ MeV. In what follows we will consider the high-energy limit. The accelerating field given by Eq. (8) is shown in Fig. 4 for the same parameters used in Fig. 2 of Ref. [4] ($\lambda=1$ μm, $w_0/\lambda=4.5$, and $w_0/\lambda=8.1$).

The axial electric field on axis can be written as the gradient of an effective potential $E_z=-Z_R^{-1}\partial U/\partial\hat{z}$, where

$$U(\hat{z})=\frac{4E_0}{k\theta}\exp\left[-\frac{(\hat{z}\theta/\theta_d)^2}{(1+\hat{z}^2)}\right]\sin\left[\phi_0-\frac{\hat{z}(\theta/\theta_d)^2}{(1+\hat{z}^2)}\right] \tag{13}$$

and the first term in Eq. (9) has been neglected, i.e., the high-energy limit. The potential in Eq. (13) is shown in Fig. 5. The change in energy of an electron traveling along the z axis with velocity approximately equal to c, injected at point z_I and extracted at z_F, is $\Delta W(z_I,z_F)=e[U(z_F)-U(z_I)]$. For the special case where $z_F=-z_I=z_0$, the energy change is

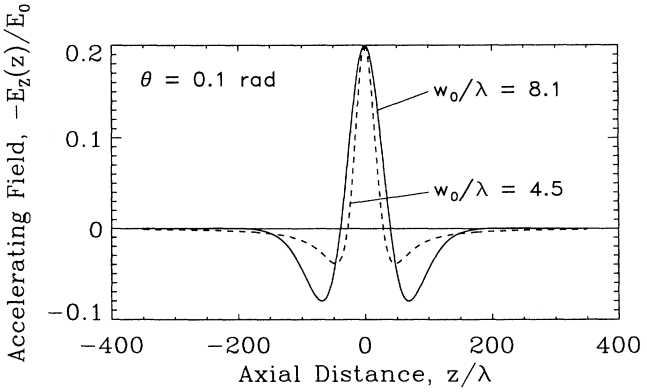

FIG. 4. Accelerating axial field $-E_z$ plotted versus position along the z axis for two crossed beams.

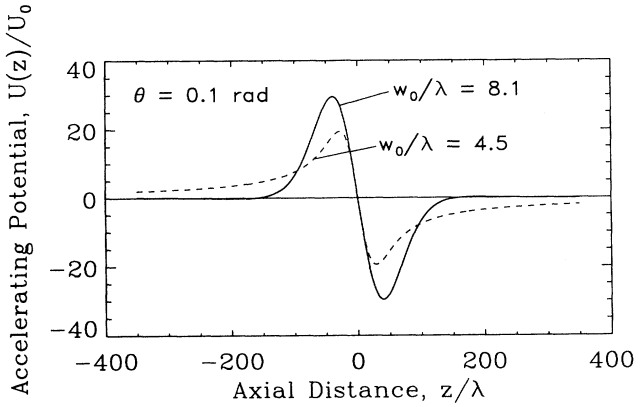

FIG. 5. Effective potential $U(z)$ plotted versus position along the z axis for two crossed beams.

$$\Delta W=\frac{8eE_0}{k\theta}\cos\phi_0\exp\left[-\frac{(\hat{z}_0\theta/\theta_d)^2}{(1+\hat{z}_0^2)}\right]\times\sin\left[\frac{\hat{z}_0(\theta/\theta_d)^2}{(1+\hat{z}_0^2)}\right]\ , \tag{14}$$

where $\hat{z}_0=z_0/Z_R$. The coefficient in Eq. (14) can be written as $8eE_0/(k\theta)=88P^{1/2}\theta_d/\theta$ MeV, where P is the laser power in TW. Note that as $z_0\to\infty$, $\Delta W\to 0$, in agreement with the LW theorem.

A finite energy gain ΔW can occur over a finite interaction range $2z_0$. The maximum energy gain occurs when $2z_0$ is equal to a slippage distance, which is the distance over which $-E_z>0$ (the width of the central peak in Fig. 4). From Eq. (14), the energy gain ΔW is maximized when z_0 satisfies

$$\tan\left[\frac{\hat{z}_0\theta^2/\theta_d^2}{1+\hat{z}_0^2}\right]=\frac{1-\hat{z}_0^2}{2\hat{z}_0}\ . \tag{15}$$

For the parameters of Ref. [4], $\lambda=1$ μm, $\theta=0.1$ rad, and $w_0/\lambda=4.5$ (8.1), we find an optimal interaction distance of $2z_0=z_s=56$ μm (79 μm), $Z_R=64$ μm (210 μm), and $\theta_d=71$ mrad (39 mrad). For a finite interaction distance $2z_0=z_s$, we find that $\Delta W(\text{MeV})=30[P(\text{TW})]^{1/2}$ for $w_0/\lambda=4.5$ and $\Delta W(\text{MeV})=26[P(\text{TW})]^{1/2}$ for $w_0/\lambda=8.1$. Hence, for $P=20$ TW, $\Delta W=130$ MeV (110 MeV) for $w_0/\lambda=4.5$ (8.1). Since the beams are tightly focused and interaction distances are very short, the accelerating field is extremely high. For example, an average accelerating gradient $\langle E_z\rangle=\Delta W/ez_s$ of $\langle E_z\rangle=2.3$ TV/m (1.4 TV/m) is obtained for $w_0/\lambda=4.5$ (8.1).

IV. HIGHER-ORDER GAUSSIAN MODES

Higher-order Gaussian modes can, in principle, provide an axial electric field component for electron acceleration in vacuum [1]. By properly choosing the electron injection point, net acceleration is possible (see Fig. 2). However, damage threshold intensities on the mirror surface place severe limits on the actual energy gain. To

examine some of the limitations associated with finite interaction regions and damage thresholds, we will consider a specific configuration of a higher-order Gaussian mode propagating along the z axis in the positive z direction, after having been reflected of a mirror located at some negative z position, as shown in Fig. 2. The results can be readily generalized to describe more complicated configurations. In the following, we consider a radially polarized, axially symmetric higher-order Gaussian TEM mode [26] given by $\mathbf{E}=E_r\mathbf{e}_r+E_z\mathbf{e}_z$, where

$$E_r=E_0\frac{rw_0}{w^2}\exp\left[-\frac{r^2}{w^2}\right]\sin\psi\ , \tag{16a}$$

$$E_z=E_0\frac{2w_0}{kw^2}\exp\left[-\frac{r^2}{w^2}\right]\times\left[\left[1-\frac{r^2}{w^2}\right]\cos\psi-\frac{zr^2}{Z_Rw^2}\sin\psi\right]\ , \tag{16b}$$

where

$$\psi=kz-\omega t+zr^2/(Z_Rw^2)-2\tan^{-1}(z/Z_R)+\phi_0\ , \tag{16c}$$

$w=w_0(1+z^2/Z_R^2)^{1/2}$ is the laser spot size, w_0 is the minimum spot size, $Z_R=\pi w_0^2/\lambda$ is the Rayleigh length, $\omega=ck$ is the frequency, and E_0 and ϕ_0 are constants. Within the paraxial approximation ($w_0\gg\lambda$), the fields in Eqs. (16) satisfy $\nabla\cdot\mathbf{E}=0$. The field components in Eqs. (16) propagate along the positive z axis, i.e., they describe the reflected fields depicted in Fig. 2, which can be used to accelerate electrons traveling in the positive z direction. The electrons are essentially unaffected by the incident fields.

An electron traveling with velocity $v_z\simeq c$ along the z axis is accelerated by the axial electric field given in Eq. (16b),

$$E_z(r=0)=2E_0\frac{w_0}{kw^2}\cos\psi_z\ , \tag{17}$$

where

$$\psi_z=-k\int dz/(2\gamma_z^2)-2\tan^{-1}(z/Z_R)+\phi_0\ , \tag{18}$$

$\gamma_z=(1-v_z^2/c^2)^{-1/2}$, and we have set $t=\int dz/v_z$. The phase velocity $v_{\rm ph}$ of the accelerating field in Eq. (17) is greater than c and therefore slips ahead of the electron. From Eq. (16c) the local phase velocity along the axis ($r=0$) is given by

$$v_{\rm ph}/c=[1-\theta_d^2/(1+\hat{z}^2)]^{-1}\ , \tag{19}$$

where $\hat{z}=z/Z_R$ and $\theta_d^2=w_0^2/Z_R^2=2/kZ_R$. Near the focal point $|z|\lesssim Z_R$,

$$v_{\rm ph}/c\simeq 1+\theta_d^2=1+1/(2\gamma_c^2)\ , \tag{20}$$

where $\gamma_c=(2\theta_d^2)^{-1/2}=\pi w_0/\sqrt{2}\lambda$ defines a critical energy. The slippage distance z_s, defined as the distance required for the electron to phase slip by π, is given approximately by $\omega z_s|v_{\rm ph}^{-1}-v_z^{-1}|\simeq\pi$, i.e.,

$$z_s\simeq\frac{\gamma_c^2\lambda}{(1+\gamma_c^2/\gamma_z^2)}=\frac{\pi Z_R/2}{(1+\gamma_c^2/\gamma_z^2)}\ . \tag{21}$$

In the high-energy limit $\gamma_z\gg\gamma_c$, slippage is dominated by diffraction, i.e., the second term in Eq. (18). In the low-energy limit $\gamma_z\ll\gamma_c$, slippage is dominated by the low velocity of the electron, i.e., the first term in Eq. (18). In the low-energy regime ($\gamma_z\ll\gamma_c$) the slippage distance is much less than a Rayleigh length ($z_s\simeq\lambda\gamma_z^2\ll Z_R$), while in the high-energy regime ($\gamma_z\gg\gamma_c$) the slippage distance is approximately a Rayleigh length ($z_s=\pi Z_R/2$).

Figure 6 shows the accelerating field as a function of axial distance for high- (solid curve) and low- (dashed curve) energy injection. In obtaining these curves, γ_z was assumed to be constant in the first term in Eq. (18) for the phase. In both cases the total area under the curves is zero, i.e., there is no net energy gain from $-\infty<z<\infty$. However, by injecting and/or extracting the electrons at a finite axial position, it is possible, in principle, to achieve net energy gain.

In the high-energy limit ($\gamma_z\gg\gamma_c$), the first term in Eq. (18) can be neglected and the accelerating axial electric field can be written as the gradient of a potential $E_z=-Z_R^{-1}\partial U/\partial\hat{z}$, where

$$U(\hat{z})=\frac{E_0w_0}{2(1+\hat{z}^2)}[(1-\hat{z}^2)\sin\phi_0-2\hat{z}\cos\phi_0]\ . \tag{22}$$

The energy gain ΔW from the injection point z_I to the extraction point z_F is given by $\Delta W=e[U(z_F)-U(z_I)]$. The maximum energy gain occurs between the points $z_I=-Z_R$ and $z_F=Z_R$ and is given by $\Delta W=eE_0w_0$. This is equal to the maximum E_z amplitude $2E_0/kw_0$, multiplied by eZ_R, i.e., the slippage distance is approximately Z_R.

On the other hand, in the low-energy limit ($\gamma_z\ll\gamma_c$), the second term in Eq. (18) can be neglected and the energy gain is given by

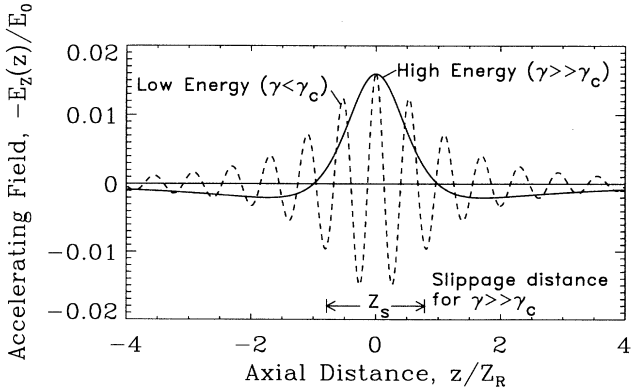

FIG. 6. Accelerating axial field $-E_z$ plotted versus position along the z axis for the higher-order Gaussian mode. The solid curve is the high-energy limit $\gamma_z\gg\gamma_c$ and the dashed curve is the low-energy limit $\gamma_z\ll\gamma_c$.

$$\frac{\Delta W}{W_F W_I} \simeq \frac{4eE_0}{m^2c^4k^2w_0}\left[\sin\left[\phi_0-\frac{k}{2}\int_{z_I}^{z_F}\frac{dz}{\gamma_z^2}\right]-\sin\phi_0\right], \tag{23}$$

where $W_{I,F}=W(z_{I,F})$, $W\simeq mc^2\gamma_z$, and $|z_{I,F}|\ll Z_R$ have been assumed. In the limit $\Delta W\ll W_I$, the maximum energy gain in the low-energy limit is $\Delta W\simeq 8eE_0\gamma_z^2/(k^2w_0)=eE_0w_0\gamma_z^2/\gamma_c^2$, which is simply the maximum field $2E_0/kw_0$ multiplied by $eZ_R(\gamma_z/\gamma_c)^2$, where $Z_R(\gamma_z/\gamma_c)^2$ is approximately equal to the slippage distance.

Hence, for a finite interaction region centered about the focus, we can write the following expression for the maximum energy gain, which is approximately valid in either the high- or low-energy limits:

$$\Delta W(\text{MeV})\simeq\frac{31[P(\text{TW})]^{1/2}}{(1+\gamma_c^2/\gamma_z^2)}, \tag{24}$$

where the average laser power is given by $P=cE_0^2w_0^2/32$. Here the critical energy $W_c\simeq mc^2\gamma_c$, where $\gamma_c\simeq\pi w_0/\sqrt{2}\lambda$, can be written as $W_c(\text{MeV})\simeq 1.1(w_0/\lambda)$. In the high-energy limit ($\gamma_z\gg\gamma_c$), the optimal interaction distance is approximately $2Z_R$, while in the low-energy limit ($\gamma_z\ll\gamma_c$), the optimal interaction distance is approximately $\lambda\gamma_z^2\ll Z_R$. In the high-energy limit, the energy gain can be substantial, i.e., $\Delta W\simeq 100$ MeV for $P=10$ TW. In the low-energy limit, however, this energy gain is reduced by the factor $\gamma_z^2/\gamma_c^2\ll 1$. Unfortunately, when damage thresholds are considered, the low-energy limit $\gamma_z\ll\gamma_c$ appears to the relevant regime for typical parameters of interest.

V. LIMITATIONS DUE TO THE DAMAGE THRESHOLD

In principle, limiting the interaction distance to a small region near the focus can lead to substantial energy gains, as discussed in the previous sections. In practice, however, the energy gain can be limited by the intensity damage threshold of the optical components. As an example, consider placing a mirror at a distance $-z_s/2$ from the focus ($z=0$) and using the higher-order Gaussian mode described in Sec. VI (see Fig. 2). A short laser pulse propagating along the $-z$ axis reflects off the mirror. At the same time, an electron beam propagating along the z axis could pass through a small hole or a thin window in the mirror such that it would interact with and be accelerated by the reflected laser pulse. The electron would gain energy as it traveled from $z=-z_s/2$ to $z_s/2$. However from $z=z_s/2$ to ∞ the electron would lose half the gained energy. The total electron energy change can be estimated by one half the maximum value given by Eq. (24).

The laser intensity on the surface of the mirror must be less than the damage threshold limit $P/(\pi w_s^2)<I_d$, where w_s is the radiation spot size on the mirror surface and I_d is the mirror damage threshold intensity. Typically, for a 1-ps laser pulse, $I_d\lesssim 5$ TW/cm^2 [25]. The damage intensity I_d increases with decreasing laser pulse duration and the precise values for ultrashort pulses $\lesssim 100$ fs are currently under investigation [25]. Since the slippage distance is much less than (approximately equal to) a Rayleigh length in the low- (high-) energy limit, the radiation spot size on the mirror is approximately the radiation waist $w_s\simeq w_0$. Hence, for a fixed laser power, the intensity at the mirror surface I_s can be made lower than I_d by increasing the focal spot size, i.e., $w_0\gtrsim(P/\pi I_d)^{1/2}$. Increasing w_0 increases the critical energy, since $\gamma_c=\pi w_0/(\sqrt{2}\lambda)$. The condition $I_s<I_d$ implies $\gamma_c^2>\pi P/(2I_d\lambda^2)$, which corresponds to a critical energy $W_c\simeq mc^2\gamma_c$ of

$$W_c(\text{GeV})\simeq\frac{6.4}{\lambda(\mu\text{m})}\left[\frac{P(\text{TW})}{I_d(\text{TW/cm}^2)}\right]^{1/2}. \tag{25}$$

Typically, this value of γ_c is quite high. For a $P=10$ TW, $\lambda=1$ μm laser and a mirror with an intensity damage threshold of $I_d=5$ TW/cm^2, we find $\gamma_c>1.8\times10^4$ such that the injected beam energy should be greater than 9 GeV to be in the high-energy limit [27]. On the other hand, if the injected energy is below this critical value, the energy gain is one-half that given by Eq. (24) with $\gamma_z\ll\gamma_c$, i.e.,

$$\Delta W(\text{MeV}) < 3.8\times10^{-7}[\lambda(\mu\text{m})]^2[W_I(\text{MeV})]^2[P(\text{TW})]^{-1/2}\times I_d(\text{TW/cm}^2), \tag{26}$$

where $W_I\simeq mc^2\gamma_z$ is the injection energy and we have used Eq. (25) for W_c. For $\lambda=1$ μm, $P=10$ TW, $I_d=5$ TW/cm^2, and $W_I=1$ GeV, the energy gain is small $\Delta W<0.6$ MeV.

Hence, when the optics are placed close to the focal point (within $\lesssim Z_R$), the intensity damage threshold requires that the minimum spot size at focus be large $w_0\gtrsim(P/\pi I_d)^{1/2}$. If one can remain in the high-energy limit $\gamma_z\gg\gamma_c$, the energy gain will remain unchanged, since $\Delta W\sim P^{1/2}$ and the total laser power is assumed to be constant. However, as the spot size w_0 increases, the critical energy increases, $\gamma_c=\pi w_0/\sqrt{2}\lambda>(\pi P/2I_d\lambda^2)^{1/2}$. For typical parameters of interest, γ_c corresponds to many GeV. When $\gamma_z\ll\gamma_c$ the energy gain is reduced $\Delta W\sim P^{1/2}\gamma_z^2/\gamma_c^2$. Although we have considered the specific example of a higher-order Gaussian mode reflecting off a mirror, these same arguments regarding the damage threshold can be applied to other laser acceleration techniques [1,2] in vacuum that rely on limiting the interaction region by using optical components.

VI. VACUUM BEAT WAVE ACCELERATION

Acceleration of electrons in vacuum can be realized using the nonlinear or ponderomotive fields associated with two laser beams. We propose a vacuum beat wave accelerator in which two laser beams of different frequencies are copropagated in the presence of an injected electron beam; see Fig. 3. Properly phased electrons, travel-

ing essentially along the same axis as the two laser beams, experience an axial acceleration from the beat term in the $\mathbf{v}\times\mathbf{B}$ force. For example, two laser beams of different frequency can be obtained by splitting a single laser pulse, frequency doubling one of the pulses, and recombining the pulses. The acceleration mechanism in the VBWA is similar to that of the inverse free electron laser [18–24]. In effect, the wiggler field in the IFEL is replaced by one of the lasers in the VBWA.

In the following analysis of the VBWA, the spot sizes of the laser beams are taken to be large compared to their wavelength and the lasers are assumed to be circularly polarized. The total laser field, represented by the vector potential, is $\mathbf{A}(z,r,t)=\mathbf{A}_1+\mathbf{A}_2$ where $\mathbf{A}_1$ and $\mathbf{A}_2$ represent laser 1 and 2, respectively,and are given by

$$\mathbf{A}_i=\frac{A_{01}w_{0i}}{w_i}\exp\left[-\frac{r^2}{w_i^2}\right](\mathbf{e}_x\cos\psi_i+\mathbf{e}_y\sin\psi_i)\ , \tag{27}$$

where

$$\psi_i=k_iz-\omega_it+r^2z/(Z_{Ri}w_i^2)-\tan^{-1}(z/Z_{Ri})+\phi_{0i}\ , \tag{28}$$

the subscript $i=1,2$ denotes the laser beam, $w_i(z)=w_{0i}(1+z^2/Z_{Ri}^2)^{1/2}$, $Z_{Ri}=\pi w_{0i}^2/\lambda_i$, $\lambda_i=2\pi c/\omega_i$, $\omega_i=ck_i$, and ϕ_{0i} is constant.

A. Basic mechanism

The basic mechanism of the VBWA can be ascertained by considering the nonlinear ponderomotive force. The axial component of the ponderomotive force F_z arising from the $-e(\mathbf{v}\times\mathbf{B}/c)$ force is

$$F_z=-\frac{mc^2}{2\gamma}\frac{\partial}{\partial z}(\mathbf{a}\cdot\mathbf{a})\ , \tag{29}$$

where $\mathbf{a}=\mathbf{a}_1+\mathbf{a}_2$, $\mathbf{a}=e\mathbf{A}/mc^2$ is the normalized laser vector potential, and γ is the electron relativistic mass factor. Substituting Eq. (27) into Eq. (29) we find that

$$F_z=\frac{mc^2}{\gamma}a_{01}a_{02}\Delta k\sin(\psi_2-\psi_1)\ , \tag{30}$$

where $\omega_2-\omega_1=\Delta\omega=c\Delta k>0$. The accelerating gradient is inversely proportional to the electron energy. The electrons will also experience an axial force from the axial component of the electric field E_z. Since E_z is zero on axis it will be neglected in this discussion. The effects of E_z, however, are included in the simulations presented in Sec. VI C.

The local phase velocity of the accelerating field, as determined by the beat wave phase $\Delta\psi=\psi_2-\psi_1$, is

$$\frac{v_{\rm ph}}{c}=\left\{1-\left[\frac{(1+\hat{z}_2^2)-(1-\hat{z}_2^2)r^2/w_{02}^2}{\Delta kZ_{R2}(1+\hat{z}_2^2)}\right]+\left[\frac{(1+\hat{z}_1^2)-(1-\hat{z}_1^2)r^2/w_{01}^2}{\Delta kZ_{R1}(1+\hat{z}_1^2)}\right]\right\}^{-1}\ , \tag{31}$$

where $\hat{z}_i=z/Z_{Ri}$. This phase velocity can be less than c and can be controlled by appropriately adjusting the wavelengths, spot sizes, and focal points of the two laser beams. Along the axis $r=0$ and near the focus of the two lasers $|z|<Z_{Ri}$, the phase velocity is

$$v_{\rm ph}/c\simeq 1-(1-Z_{R1}/Z_{R2})/(\Delta kZ_{R1})\ , \tag{32}$$

where $\Delta kZ_{Ri}\gg 1$ has been assumed. Notice that $v_{\rm ph}<c$ for $Z_{R2}>Z_{R1}$. The relativistic factor associated with the phase velocity $\gamma_{\rm ph}=(1-v_{\rm ph}^2/c^2)^{-1/2}$ is

$$\gamma_{\rm ph}\simeq\left[\frac{\Delta kZ_{R1}/2}{1-Z_{R1}/Z_{R2}}\right]^{1/2}\ , \tag{33}$$

which can be tuned to the electron injection energy by appropriately choosing the laser parameters. The slippage distance z_s, which is the distance over which an electron phase slips by an amount of π with respect to the beat wave, i.e., $\Delta\omega z_s|v_z^{-1}-v_{\rm ph}^{-1}|\simeq\pi$, is

$$z_s\simeq 2\pi\gamma_z^2Z_{R1}/|\Delta kZ_{R1}-2\gamma_z^2(1-Z_{R1}/Z_{R2})|\ , \tag{34}$$

which can be made large by approximately choosing the laser parameters.

The acceleration distance is limited not by the slippage distance but by the diffraction range, i.e., Rayleigh length. For a properly phased electron, the rate of change of energy is $dW/dt=cF_z$ and the maximum energy change is

$$dW/dz=a_{01}a_{02}\Delta kmc^2/(1+W/mc^2)\ , \tag{35}$$

where we have set $\sin(\psi_2-\psi_1)=1$ and $W=mc^2(\gamma-1)$ is the electron energy. For the purposes of illustration we set $a_{01}=a_{02}=a_0, Z_{R1}=Z_{R2}=Z_R$, and take the effective acceleration range to be two Rayleigh lengths. Equation (35) yields

$$W_F=[W_I^2+8\pi^2(a_0w_{01}/\lambda_1)^2(\lambda_1/\lambda_2-1)m^2c^4]^{1/2}\ , \tag{36}$$

where W_F (W_I) is the final (initial) electron energy and we assumed $W_I\gg mc^2$. For circularly polarized radiation, the laser power is given by $P_i({\rm TW})=0.043(a_{0i}w_{0i}/\lambda_i)^2$. The final energy can be written as $W_F^2=W_I^2+480(\lambda_1/\lambda_2-1)P_1$, where the energies $W_{I,F}$ are in MeV and the laser power P_1 is in TW.

In the above analysis, it was assumed that the electrons remain close to the z axis. However, the electrons undergo transverse oscillations as they are accelerated along the z axis. The magnitude of the transverse oscillations, which must be much less than the laser spot size, can be estimated for a highly relativistic electron. In the presence of a single laser beam the transverse oscillation Δx is given by $d\Delta x/dt=(ca/\gamma)\cos\psi$, where $\psi\simeq(k-Z_R^{-1})z-kct$. By setting $t=z/v_z$, the wave number of the transverse oscillation is given approximately by $k_{\rm osc}\simeq 1/Z_R$ for $2\gamma_z^2\gg kZ_R$ and $k_{\rm osc}\simeq k/2\gamma_z^2$ for $2\gamma_z^2\ll kZ_R$. An estimation of the maximum electron oscillation amplitude is given by

$$\frac{\Delta x_{\rm max}}{w_0}\simeq\frac{a_0\alpha}{\gamma_\perp(1+\alpha^2)}\ , \tag{37}$$

where $\alpha^2=kZ_R/(2\gamma_z^2)=(\pi w_0/\gamma_z\lambda)^2$ and $\gamma_\perp$

$=(1+a_0^2)^{1/2}$. In order for the electrons to remain in the high-intensity fields, it is necessary that $\Delta x_{\max}/w_0 < 1$.

B. Radiative losses

A limit to the maximum energy attainable in the VBWA is imposed by radiative losses. As the electrons interact with the laser fields, they will undergo transverse quiver oscillations, which will cause the electrons to radiate. The power radiated by a single electron P_R is given by the relativistic Larmor formula [28]

$$P_R = \frac{2e^2\gamma^2}{3c}\left[\left[\frac{d\mathbf{u}}{dt}\right]^2 - \left[\frac{d\gamma}{dt}\right]^2\right], \tag{38}$$

where $\mathbf{u}=\mathbf{p}/mc$ is the normalized electron momentum. It can be shown that the power radiated is determined primarily by the transverse motion of the electron in the laser field. In the one-dimensional limit ($w_0 \gg \lambda$), conservation of canonical momentum implies $\mathbf{u}_\perp = \mathbf{a}_\perp$, where $\mathbf{a}_\perp = a_x\mathbf{e}_x + a_y\mathbf{e}_y$. For a single laser beam

$$P_R \simeq \frac{2}{3} r_e mc^3 \gamma^2 a_0^2 k^2 \left[\frac{1}{2\gamma_z^2} + \frac{1}{kZ_R}\right]^2, \tag{39}$$

where $r_e = e^2/mc^2$ is the classical electron radius. Including this term in the equation for evolution of the electron energy Eq. (35) gives

$$\frac{d\gamma}{dz} \simeq a_{01}a_{02}\frac{\Delta k}{\gamma} - \frac{2}{3} r_e \gamma^2 \left[\frac{a_{01}^2}{Z_{R1}^2} + \frac{a_{02}^2}{Z_{R2}^2}\right], \tag{40}$$

where $\gamma_z^2 \gg k_i Z_{Ri}/2$ has been assumed. Setting $d\gamma/dz = 0$ gives a maximum value for γ. Assuming $\Delta k = k_1$, $a_{01} = a_{02}$, and $Z_{R1} = Z_{R2}$, the maximum electron energy is given by

$$W_{\max} \simeq \pi mc^2 (w_{01}/\lambda_1)(3w_{01}/2r_e)^{1/3} \tag{41}$$

or $W_{\max} \simeq 1.3(w_{01}^{4/3}/\lambda_1)$, where $W_{\max}$ is in GeV and w_{01} and λ_1 are in μm. As an example, for $w_{01} = 10$ μm and $\lambda_1 = 1$ μm, $W_{\max} \simeq 28$ GeV.

C. Single-particle simulations

To verify the basic mechanism of the VBWA, single-particle simulations were performed. These simulations are based on model equations derived from the relativistic Lorentz force equation, which can be written as

$$d\mathbf{u}/dt = \partial\mathbf{a}/\partial t - (c\mathbf{u}/\gamma)\times(\nabla\times\mathbf{a}), \tag{42}$$

where $\mathbf{u}=\mathbf{p}/mc$ is the normalized electron momentum. The evolution of the electron energy is described by

$$d\gamma/dt = (\mathbf{u}/\gamma)\cdot\partial\mathbf{a}/\partial t, \tag{43}$$

where $\gamma = (1+u^2)^{1/2}$. For the fields in Eq. (27), $a^2 = \mathbf{a}\cdot\mathbf{a}$ is given by

$$a^2 = \hat{a}_1^2 + \hat{a}_2^2 + 2\hat{a}_1\hat{a}_2\cos(\psi_2-\psi_1) + a_z^2, \tag{44}$$

where $\hat{a}_i = (a_{0i}w_{0i}/w_i)\exp(-r^2/w_i^2)$. The axial component of the field is given by $\nabla\cdot\mathbf{a}=0$,

$$a_z = \sum_{i=1,2} \frac{2\hat{a}_i}{k_i w_i^2}[(x-\hat{z}_i y)\sin\psi_i - (\hat{z}_i x + y)\cos\psi_i], \tag{45}$$

where $w_{0i} \gg \lambda_i$ has been assumed. For a sufficiently broad laser pulse ($w_{0i} \gg \lambda_i$), the transverse canonical momentum of the electrons is approximately conserved. This also assumes that the transverse quiver motion, i.e., the first term on the right-hand side of Eq. (42), $\partial a_\perp/\partial t$, is much greater than the radial ponderomotive force F_r, i.e., the second term on the right-hand side of Eq. (42), $F_r \sim -(1/2\gamma)\nabla_\perp a^2$, which is small for typical VBWA parameters. Hence $\mathbf{u}_\perp \simeq \mathbf{a}_\perp$, which assumes that far from the laser focus the initial transverse velocity of the electron is zero. The electron energy is then determined by the equation

$$\frac{d\gamma}{dz} \simeq \frac{\hat{a}_1\hat{a}_2}{\gamma\beta_z}\Delta k \sin(\psi_2-\psi_1) - \sum_{i=1,2}\frac{2\hat{a}_i}{w_i^2}[(x-\hat{z}_i y)\cos\psi_i + (\hat{z}_i x + y)\sin\psi_i]. \tag{46}$$

The transverse orbits are given by

$$\frac{dx}{dz} \simeq \frac{1}{\gamma\beta_z}\sum_{i=1,2}\hat{a}_i\cos\psi_i, \tag{47a}$$

$$\frac{dy}{dz} \simeq \frac{1}{\gamma\beta_z}\sum_{i=1,2}\hat{a}_i\sin\psi_i, \tag{47b}$$

where $\gamma = \gamma_z\gamma_\perp$, $\gamma_z = (1-\beta_z^2)^{-1/2}$, $\beta_z = v_z/c$, and $\gamma_\perp = (1+a_x^2+a_y^2)^{1/2}$. Since z is the independent variable, $t = \int dz/v_z$ is used in the expression for each phase ψ_i, Eq. (28).

Analytical solutions to Eq. (46) can be found in the high-energy limit for electrons that remain near the axis. Setting $x = y = 0$ and $t = z/c$ and assuming $Z_{R1} = Z_{R2}$, the electron energy is given by

$$\gamma_F^2 - \gamma_I^2 = 2a_{01}a_{02}\Delta k Z_R \sin(\phi_{02}-\phi_{01}) \times(\tan^{-1}\hat{z}_F - \tan^{-1}\hat{z}_I), \tag{48}$$

where $\gamma_{I,F} = \gamma(z = z_{I,F})$. For the case of an infinite interaction region $z_I = -\infty$ and $z_F = \infty$, the electron energy is given by $\gamma_F^2 - \gamma_I^2 = 2\pi a_{01}a_{02}\Delta Z_R$, assuming $\sin(\phi_{02}-\phi_{01}) = 1$. Letting $a_{02} = a_{01}$, the electron energy $W \simeq mc^2\gamma$ can be written in terms of the laser power $P_1(\text{TW}) = 0.043(a_{01}w_{01}/\lambda_1)^2$ as

$$W_F(\text{MeV}) = \{[W_I(\text{MeV})]^2 + 750(\lambda_1/\lambda_2 - 1)P_1(\text{TW})\}^{1/2}, \tag{49}$$

which is in approximate agreement with the estimate given in Sec. VI A.

Equation (49) is the energy gain from the ponderomotive term only, i.e., the first term on the right-hand side of Eq. (46). The particle was assumed to remain on axis ($x = y = 0$), hence the effects of the axial electric field E_z, represented by the summation term on the right-hand side of Eq. (46), were neglected. However, the transverse electric field produces transverse electron oscillations and

the effects of E_z can be significant. In the high-energy limit $2\gamma_z^2 \gg kZ_R$, the magnitude of the transverse orbits can be large, i.e., $x,y \sim a_0 Z_R/\gamma$. This implies that the axial field terms in Eq. (46), which are proportional to x and y, can be as large as the ponderomotive term.

The theoretical energy gain of Eq. (49) and the importance of the axial field terms in Eq. (46) can be verified by single-particle simulations. In these simulations, the model equations (46) and (47) are solved numerically. Here we consider a particle with an injection energy of $W_I \simeq 50$ MeV ($\gamma_I = 100$) copropagating with two high-intensity laser pulses. The lasers have wavelengths $\lambda_1 = 1$ μm and $\lambda_2 = 0.5$ μm and spot sizes $w_{01} = 10$ μm and $w_{02} = w_{01}/\sqrt{2}$. As in Eq. (49), $Z_{R1} = Z_{R2} = Z_R$ and $a_{01} = a_{02} = a_0$. An intensity parameter of $a_0 = 1.53$ was chosen such that lasers 1 and 2 have power 10 and 20 TW, respectively. The final energy predicted by Eq. (49) is $W_F \simeq 100$ MeV for these parameters.

Simulations were performed with and without the effects of the axial electric field E_z, i.e., with and without the summation term on the right-hand side of Eq. (46). These results are shown in Fig. 7, in which the particle energy is plotted versus axial position z. The solid line shows the evolution of the electron energy including the effects of E_z, i.e., all terms are kept on the right-hand side of Eq. (46). The dashed line shows the electron energy neglecting the effects of E_z, i.e., only the first term is kept on the right-hand side of Eq. (46). In these simulations, input phases ϕ_{01} and ϕ_{02} are chosen such that $\psi_2 - \psi_1 \simeq \pi/2$ at $z = 0$, which maximizes the acceleration near focus. Simulations were performed over the region $-30Z_R < z < 30Z_R$, where $Z_R \simeq 0.31$ mm. The solid line ($E_z \neq 0$) gives a final energy of $W_F \simeq 93$ MeV and the dashed line ($E_z = 0$) gives $W_F \simeq 90$ MeV. Both are somewhat less than the theoretical estimate, which assumes $x = y = 0$. As the electron oscillates off axis, the laser field amplitude is reduced, $\hat{a} \sim a_0 \exp(-r^2/w_0^2)$, thus reducing the ponderomotive acceleration. Furthermore, the transverse oscillation of the electron is such that the E_z terms in Eq. (46), proportional to x and y, contribute significantly to the acceleration of the electron. This results in the oscillatory behavior of the energy near the origin and a slightly higher final energy, as shown by the solid curve in Fig. 7. The average accelerating gradient observed over the entire $60Z_R$ simulation region is $(W_F - W_I)/60Z_R \simeq 50$ GeV/m.

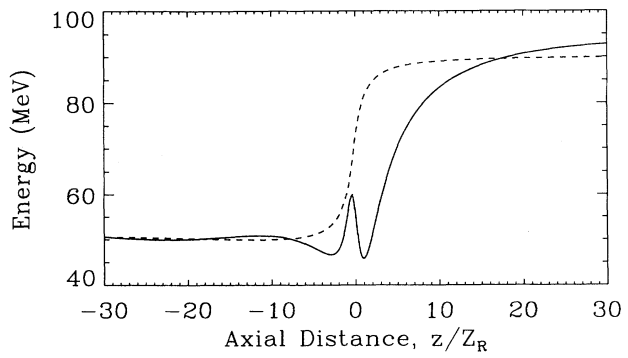

FIG. 7. Particle energy versus axial position z from the complete model equations (solid line) and with the effects of E_z neglected, i.e., the second term in Eq. (46) is dropped (dashed line).

VII. DISCUSSION

Electron acceleration by laser fields in vacuum is subject to the LW theorem [13–15], which states that the net energy gain of a highly relativistic electron interacting with an electromagnetic field in vacuum is zero. However, a net energy gain can be obtained by violating one or more of the assumptions of the LW theorem. We have shown that the concept of using two crossed laser beams in vacuum to accelerate electrons obeys the LW theorem [5], i.e., a highly relativistic electron traveling from $z = -\infty$ to ∞ achieves zero net acceleration.

A relativistic electron can obtain a net energy gain if the interaction distance is limited to a slippage distance z_s about the focal point of the laser fields. Typically, $z_s \lesssim Z_R$. To limit the interaction region, optical components are needed relatively close ($\lesssim Z_R$) to the focal point. This, however, may be impractical due to the high-intensity requirement on the laser field and the relatively low damage threshold of typical optical components. We examined the specific case of electron acceleration by a higher-order Gaussian-mode laser, which is reflected by a mirror placed a distance $|z_s/2|$ from focus. The maximum energy gain of the electron is given by Eq. (24), i.e., $\Delta W \simeq 31 P^{1/2}/(1 + W_c^2/W_I^2)$, where ΔW is in MeV, P is in TW, and $W_c(\text{MeV}) \simeq w_0/\lambda$ is the critical energy. For substantial energy gains, the injection energy must exceed the critical energy. For a fixed laser power P, limiting the intensity at the mirror surface to a value below the damage threshold I_d implies a large focal spot size w_0, i.e., $w_0 \geq (P/\pi I_d)^{1/2}$. This implies a large value for the critical energy. For $W_I \ll W_c$, the energy gain ΔW is greatly reduced. A similar argument can be applied to other configurations [1,2] that rely on electron acceleration by the axial laser field E_z over a limited interaction region near the laser focus.

We have proposed a vacuum beat wave accelerator in which two laser beams of different frequencies are copropagated in the presence of an injected electron beam. Properly phased electrons, traveling essentially along the same axis as the two laser beams, experience an axial acceleration from the beat term in the $\mathbf{v} \times \mathbf{B}$ force. Since the VBWA relies on the nonlinear ponderomotive forces associated with the $\mathbf{v} \times \mathbf{B}$ term, it violates the assumptions of the LW theorem. Hence the VBWA can lead to substantial energy gains, even in the limit of an infinite interaction region. The VBWA has the further advantage that, by appropriately choosing the wavelengths, spot sizes, and focal points of the two lasers, the phase velocity v_{ph} of the beat wave can be adjusted. By tuning the phase velocity to obtain $v_{\text{ph}} < c$ in the vicinity of the laser focus, phase slippage can be reduced. The validity of the VBWA mechanism was confirmed by performing single-particle simulations.

The maximum energy gain in the VBWA accelerator is given by Eq. (49). For $W_I \leq \Delta W$ and $\Delta k \simeq k_1$, $\Delta W(\mathrm{MeV}) \simeq 27[P_1(\mathrm{TW})]^{1/2}$. It is insightful to compare this to a plasma-based, laser-driven accelerator, such as the laser wake field accelerator (LWFA). For a LWFA in the standard configuration [10–12], i.e., using a single laser pulse with a pulse length L equal to the plasma wavelength and assuming that the laser pulse undergoes vacuum diffraction, the energy gain is given by $\Delta W(\mathrm{MeV}) \simeq 580(\lambda/L)P(\mathrm{TW})$. Hence, for equal powers $P_1 = P$, the single-stage energy gain in the VBWA can be greater than that in the standard LWFA for $P_1(\mathrm{TW}) < (L/21\lambda)^2$, e.g., $P_1 < 27$ TW for $\lambda = 1$ μm and $L/c = 0.5$ ps. For $P_1 = 27$ TW, $\Delta W \simeq 140$ MeV. This demonstrates that, for single-stage energy gains in the 100-MeV regime, the VBWA is comparable to other laser-driven accelerator schemes.

ACKNOWLEDGMENTS

The authors acknowledge useful conversations with D. Sutter and the assistance of A. Ting. This work was supported by the Department of Energy and the Office of Naval Research.

[1] E. J. Bochove, G. T. Moore, and M. O. Scully, Phys. Rev. A **46**, 6640 (1992); M. O. Scully and M. S. Zubairy, *ibid.* **44**, 2656 (1991).

[2] L. C. Steinhauer and W. D. Kimura, J. Appl. Phys. **72**, 3237 (1992).

[3] T. Hauser, W. Scheid, and H. Hora, in *Laser Interaction and Related Plasma Phenomena,* edited by G. H. Miley, AIP Conf. Proc. No. 318 (AIP, New York, 1994), p. 20.

[4] C. M. Haaland, Opt. Commun. **114**, 280 (1995).

[5] P. Sprangle, E. Esarey, J. Krall, and A. Ting, Opt. Commun. (to be published).

[6] E. Esarey, P. Sprangle, M. Pilloff, and J. Krall, J. Opt. Soc. Am. B **12**, 1695 (1995).

[7] P. Maine, D. Strickland, P. Bado, M. Pessot, and G. Mourou, IEEE J. Quantum Electron. **24**, 398 (1988); G. Mourou and D. Umstadter, Phys. Fluids B **4**, 2315 (1992).

[8] M. D. Perry and G. Mourou, Science **264**, 917 (1994).

[9] C. E. Clayton, K. A. Marsh, A. Dyson, M. Everett, A. Lal, W. P. Leemans, R. Williams, and C. Joshi, Phys. Rev. Lett. **70**, 37 (1993).

[10] T. Tajima and J. M. Dawson, Phys. Rev. Lett. **43**, 267 (1979).

[11] L. M. Gorbunov and V. I. Kirsanov, Zh. Eksp. Teor. Fiz. **93**, 509 (1987) [Sov. Phys. JETP **66**, 209 (1987)].

[12] P. Sprangle, E. Esarey, A. Ting, and G. Joyce, Appl. Phys. Lett. **53**, 2146 (1988); E. Esarey, P. Sprangle, J. Krall, A. Ting, and G. Joyce, Phys. Fluids B **5**, 2690 (1993).

[13] J. D. Lawson, Rutherford Laboratory Report No. RL-75-043, 1975 (unpublished); IEEE Trans. Nucl. Sci. **NS-26**, 4217 (1979).

[14] P. M. Woodward, J. Inst. Electr. Eng. **93**, 1554 (1947).

[15] R. B. Palmer, in *Frontiers of Particle Beams,* edited by M. Month and S. Turner, Lecture Notes in Physics Vol. 296 (Springer-Verlag, Berlin, 1988), p. 607; Part. Accel. **11**, 81 (1980).

[16] W. D. Kimura, G. H. Kim, R.D. Romea, L. C. Steinhauer, I. V. Pogorelsky, K. P. Kusche, R. C. Fernow, X. Wang, and Y. Liu, Phys. Rev. Lett. **74**, 546 (1995).

[17] J. R. Fontana and R. H. Pantell, J. Appl. Phys. **54**, 4285 (1983).

[18] A. A. Kolomenskii and A. N. Lebedev, Zh. Eksp. Teor. Sov. Phys. JETP **23**, 733 (1966).

[19] R. B. Palmer, J. Appl. Phys. **43**, 3014 (1972).

[20] P. Sprangle and C. M. Tang, Nucl. Sci. **NS-28**, 3346 (1981).

[21] R. H. Pantell and T. I. Smith, Appl. Phys. Lett. **40**, 753 (1982).

[22] E. D. Courant, C. Pellegrini, and W. Zakowicz, Phys. Rev. A **32**, 2813 (1985).

[23] A. C. Ting and P. Sprangle, Part. Accel. **22**, 149 (1987).

[24] T. B. Zhang and T. C. Marshall, Phys. Rev. E **50**, 1491 (1994).

[25] D. Du, X. Liu, G. Korn, J. Squier, and G. Mourou, Appl. Phys. Lett. **64**, 3071 (1994); B. C. Stuart, M. D. Feit, A. M. Rubenchik, B. W. Shore, and M. D. Perry, Phys. Rev. Lett. **74**, 2248 (1995).

[26] P. W. Milonni and J. H. Eberly, *Lasers* (Wiley, New York, 1988), Chap. 14; A. Yariv, *Quantum Electronics,* 3rd ed. (Wiley, New York, 1989), Chap. 6.

[27] The damage threshold, often expressed in terms of the laser fluence $F_d = I_d \tau_L$, is a function of the laser pulse duration τ_L. The critical electron energy γ_c and minimum laser spot size at the mirror surface w_0 are given by $\gamma_c^2 > \pi P \tau_L/(2F_d\lambda^2)$ and $w_0^2 > P\tau_L/(\pi F_d)$. Recent experiments [25] suggest that for τ_L less than a few picoseconds, F_d may increase (or remain constant) as τ_L decreases. This implies that for a fixed peak laser power, γ_c and w_0 can be reduced by reducing τ_L.

[28] J. D. Jackson, *Classical Electrodynamics,* 2nd ed. (Wiley, New York, 1975), p. 660.